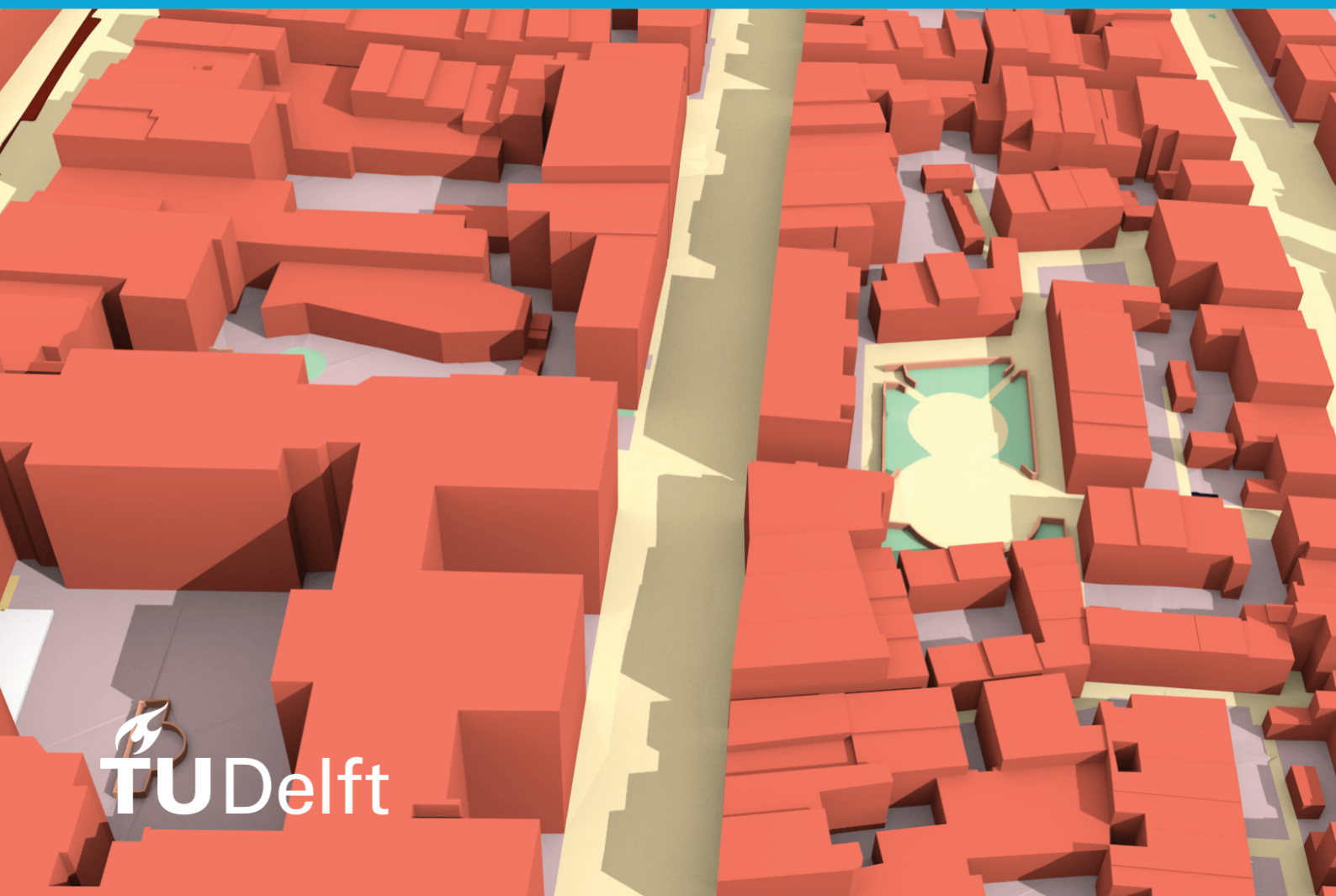


Additional thesis in Water Management

# Simulation of Greenhouse Tomato Crop Transpiration Using Two Theoretical Models

Ying Yin

2023





**Additional thesis in Water Management**

**Simulation of Greenhouse Tomato Crop  
Transpiration Using Two Theoretical  
Models**

Ying Yin

May 2023

Ying Yin: *Simulation of Greenhouse Tomato Crop Transpiration Using Two Theoretical Models*  
(2023)

The work in this thesis was carried out in the:

Delft University of Technology

Supervisors: Prof. Marie-Claire ten Veldhuis

Co-reader:

# Abstract

Water consumption reduction in greenhouse cultivation is a key objective for growers to optimize resource usage. Accurate estimation of transpiration, enabling growers to adapt water inputs to exact plant requirements, is vital for efficient water management. Various models have been developed to estimate transpiration. The Penman-Monteith and Stanghellini models are two of the most widely used models.

The Penman-Monteith model was originally designed for open-field conditions, while the Stanghellini model was specifically developed for greenhouse environments. In this study, the accuracy of these models in estimating transpiration was evaluated by comparing their estimated values with measured transpiration data. By affecting the VPD and stomatal resistance, temperature directly impacts the rate of transpiration in plants. This research also addresses a significant gap in previous studies by determining the optimal observation height for temperature data, which is essential for accurate modeling of transpiration.

Linear regression analysis was employed to assess the performances of the models. The results show that the Stanghellini model provides more precise estimations of transpiration compared to the Penman-Monteith model under greenhouse conditions. Moreover, using temperatures measured above the top of the plant canopy improves the accuracy of transpiration estimations in both models. Enhancing the accuracy of transpiration models in greenhouse conditions is critical for promoting efficient water management practices.

# Contents

<b>1. Introduction</b>	<b>1</b>
1.1. Model Characteristics . . . . .	1
1.2. Comparison between Transpiration Models . . . . .	3
1.3. Objectives of the Study . . . . .	4
<b>2. Methodology</b>	<b>5</b>
2.1. Transpiration Model Theory . . . . .	5
2.1.1. Penman-Monteith model . . . . .	5
2.1.2. Stanghellini model . . . . .	6
2.1.3. Aerodynamic Resistance . . . . .	6
2.1.4. Canopy Resistance . . . . .	8
2.2. Experimental Method . . . . .	9
2.2.1. Experimental Setup . . . . .	10
2.2.2. Microclimate Measurement . . . . .	10
2.2.3. Leaf Area Index Measurement . . . . .	12
2.2.4. Transpiration Measurement . . . . .	12
2.3. Data Processing . . . . .	14
2.3.1. Irrigation and Drainage . . . . .	14
2.3.2. Water Storage . . . . .	14
2.3.3. Sap Flow . . . . .	15
2.3.4. Radiation and Temperature . . . . .	15
2.4. Evaluation of Model Performance . . . . .	15
<b>3. Result</b>	<b>16</b>
3.1. Water Balance Model and Sap Flow . . . . .	16
3.2. Microclimate Conditions . . . . .	18
3.2.1. Microclimate Data Measured by the Porometer . . . . .	18
3.2.2. Microclimate Data Measured by Other Devices . . . . .	19
3.3. Aerodynamic and Canopy Resistance . . . . .	20
3.3.1. Aerodynamic Resistance . . . . .	21
3.3.2. Canopy Resistance . . . . .	21
3.4. Application of the Penman-Monteith model and the Stanghellini model . . . . .	22
3.5. Selection of the Optimal Temperature Measurement Locations . . . . .	24
3.5.1. Temperature Used in the Penman-Monteith model . . . . .	24
3.5.2. Temperature Used in the Stanghellini model . . . . .	25
<b>4. Discussion</b>	<b>26</b>
<b>5. Conclusion</b>	<b>29</b>
<b>A. Appendix</b>	<b>31</b>
A.1. Greenhouse Setup . . . . .	31

A.2. Air Properties . . . . . 31  
A.3. Selection of the Optimal Temperature Measurement Locations . . . . . 32

# List of Figures

2.1. Devices for Measuring Microclimate Parameters . . . . .	11
2.2. Water Balance in the Slab . . . . .	13
3.1. Modelled Transpiration (Water Balance) and Sap Flow . . . . .	16
3.2. Cumulative Graph) . . . . .	17
3.3. Relationship between Daily Transpiration and Sap Flow . . . . .	18
3.4. Humidity and Temperature Measured by Porometer . . . . .	19
3.5. Air Temperature Measured by LAT Sensors Plant 2B, at Height 0.3 and 2.3 <i>m</i> .	19
3.6. Leaf Temperature Measured by LAT Sensors Plant 2B, at Height 0.3 and 2.3 <i>m</i>	20
3.7. Radiation Measurement . . . . .	20
3.8. Aerodynamic and Canopy Resistance . . . . .	21
3.9. Aerodynamic Resistance and Air-to-Leaf Temperature Difference . . . . .	21
3.10. Canopy Resistance . . . . .	22
3.11. Comparison between measured and estimated transpiration (T at top of plants)	23
3.12. Relationship between Sap Flow and Modelled Transpiration . . . . .	23
3.13. Violin Graph . . . . .	24
A.1. Slab . . . . .	31
A.2. 0.3 <i>m</i> from plant roots . . . . .	32
A.3. 0.9 <i>m</i> from plant roots . . . . .	33
A.4. 1.5 <i>m</i> from plant roots . . . . .	33
A.5. 2.1 <i>m</i> from plant roots . . . . .	34
A.6. 2.7 <i>m</i> from plant roots . . . . .	35
A.7. 3.3 <i>m</i> from plant roots . . . . .	35



# List of Tables

1.1. Location of the Climatic Parameters Used in Studies . . . . .	2
1.2. Detail . . . . .	3
1.3. Results of Different Transpiration Models . . . . .	4
2.1. Expression of the Nusselt number ( $N_u$ ) . . . . .	8
2.2. Values of $c_1$ to $c_4$ . . . . .	9
2.3. Devices for Measuring Microclimate Parameters . . . . .	12
2.4. Devices for Measuring Microclimate Parameters . . . . .	14
3.1. Daily Modelled Transpiration and Sap Flow . . . . .	17
3.2. Correlation between Measured and Simulated Transpiration Rates (PM) . . . . .	25
3.3. Correlation between Measured and Simulated Transpiration Rates (SM) . . . . .	25
A.1. Air Properties . . . . .	32

# Acronyms

<b>PM</b>	Penman-Monteith model . . . . .	1
<b>SM</b>	Stanghellini model . . . . .	1
<b>LAI</b>	leaf area index . . . . .	1
$E_t$	transpiration . . . . .	5
$R_n$	net radiation . . . . .	9
$\lambda$	latent heat flux of vaporisation	
$C_p$	specific heat of air at constant pressure	
$\rho$	density of water	
$\rho_a$	density of air . . . . .	32
$e_a$	actual vapour pressure of the air	
$e_s$	saturated vapour pressure of the air	
$\gamma$	psychrometer constant	
$r_a$	aerodynamic resistance . . . . .	6
$r_c$	canopy resistance . . . . .	3
$s$	slope of the saturated vapour pressure curve . . . . .	6
$T$	temperature . . . . .	5
$h_s$	heat exchange coefficient . . . . .	6
$N_u$	Nusselt number . . . . .	ix
$\lambda_a$	air thermal conductivity	
$l$	characteristic dimension of the leaf . . . . .	7
$L$	length of the leaf	
$W$	Width of the leaf	
<b>Re</b>	Reynolds number . . . . .	7
<b>Gr</b>	Grashof number . . . . .	7
$u$	wind speed	
$\mu_a$	air dynamic viscosity . . . . .	32
$g$	acceleration of gravity	
$\beta$	volumetric thermal expansion coefficient of air . . . . .	32
$\Delta T$	temperature difference between the leaf temperature and the air temperature	
$r_{c, min}$	minimum canopy resistance	
<b>VPD</b>	vapour pressure deficit . . . . .	9
$T_a$	air temperature . . . . .	10
$T_l$	leaf temperature . . . . .	10
$h$	relative humidity . . . . .	10
$Q_{in}$	incoming water flux	
$Q_{out}$	outgoing water flux	
<b>S</b>	storage	
<b>I</b>	irrigation	
<b>D</b>	drainage	
<b>WE</b>	water extraction by plant roots	
$S_{soil}$	soil moisture storage	
$S_{plant}$	water stored in the plants for growth	

$R^2$	Coefficient of Determination . . . . .	3
$C_i$	calculated transpiration	
$M_i$	measured transpiration	
$\bar{M}$	average measured transpiration	



# 1. Introduction

Greenhouse cultivation has become a popular farming system globally owing to its ability to provide a controlled environment that is conducive for optimum crop production, thereby leading to high profits. Greenhouses are of great importance in the food supply of high-latitude countries [25]. The irrigation system is a vital greenhouse farming component affecting crop yield and quality [19]. A thorough understanding of the transpiration process is essential for adapting water inputs to meet plant needs. Therefore, various models have been developed to predict plant transpiration. The Penman-Monteith model (*PM*) and Stanghellini model (*SM*) models are two widely used models in greenhouse conditions.

## 1.1. Model Characteristics

The *PM* model, developed by Penman in 1948 [17] and refined by Monteith in 1965 [13], is widely used for estimating crop transpiration in open fields. This estimation is crucial for effective water management in agricultural systems. The *PM* model incorporates a 'big-leaf' approach, where the vegetation is simplified to a single leaf, with one idealized stomatal cavity [12]. This simplification allows for practical estimation of transpiration rates within the model. Furthermore, based on the perfectly mixed-tank approach, this method assumes thermodynamic homogeneity within both the canopy and the air above the plants [15]. The *PM* model therefore expresses crop transpiration as a function of net radiative flux and vapour pressure deficit at a particular temperature. Microclimate data used for *PM* model calculations, such as temperature, humidity, wind speed, and radiation, are typically collected at a single point located above the crop in the greenhouse (Table 1.1).

Stanghellini [21] further improved the *PM* model for greenhouse applications by incorporating the crop leaf area index (*LAI*), which represents the total leaf surface area per unit of ground area. This modification allows the model to take into account the effects of canopy shading and light interception, which may strongly influence crop transpiration rates in greenhouses where light conditions may be more variable than in open fields [11]. This model typically uses microclimate data measured within the canopy or above the crop (Table 1.1). The reliability of transpiration predictions by various models largely depends on the measurement positions of microclimatic data [26]. Despite the importance of measurement positions, Table 1.1 reveals that authors frequently omit information on the exact locations of microclimatic data used in the *PM* and *SM* models.

Table 1.1.: Location of the Climatic Parameters Used in Studies

	Model	Leaf temperature	Air temperature	Humidity	Radiation	Air speed
Jolliet and Bailey [9]	SM	2 levels	Inside the crop	Inside the crop	$R_s$ outside the greenhouse	Inside the crop
Bailey et al. [4]	PM/SPM	Underside of 4 leaves	Above the crop	Above the top	$R_s, R_n$ inside greenhouse	Above the crop
Caspari et al. [5]	PM	Not measured	Above the crop	Above the crop	$R_s, R_n$ above the crop	Above the crop
Prenger et al. [18]	PM/SM	Not measured	Above and inside the crop	Above and inside the crop	$R_{s,in}$ above the crop	Near the crop
Acquah et al. [1]	SM	Not measured	Above and inside the crop	Above and inside the crop	$R_{s,in}, R_n$ above the crop	Above the crop
Yan et al. [26]	SM	By infrared thermometer, without further information	Above and inside the crop	Above and inside the crop	$R_n$ above the crop	Above the crop
Zheng et al. [27]	PM	Not measured	Inside the greenhouse	Inside the greenhouse	$R_s, R_n$ inside the greenhouse	Not measured
Harms [8]	PM/SM	6 leaves at the same height	Inside the crop	Inside the crop	$R_n$ above the crop	Above the crop
Shao et al. [20]	PM	Not measured	Above the crop	Above the crop	$R_n$ above the crop	Above the crop

Table 1.2.: Detail

	type of crop	greenhouse condition	time-scale and period of comparison
Jolliet and Bailey [9]	tomato	wind tunnel and full-size greenhouse	9.5h, 15h, 17h
Bailey et al. [4]	Ficus benjamina	IRTA Spain and Silsoe UK	average value of every 5min in 20 hours
Caspari et al. [5]	Asian pears	well-watered and water-stressed	averaged every 2h from before sunrise to 20:30h in 4 months
Prenger et al. [18]	Red maple tree	controlled-environment greenhouse	in one day (24h), each data point is an average of 14 days, recorded every 15min
Prenger et al. [18]	tomato	unheated and naturally ventilated greenhouse multi-span Venlo-type greenhouse	from March 2016 to July 2016, data recorded every 10s and averaged every 10min
Yan et al. [26]	cucumber	Venlo-type glasshouse oriented east to west; humid, subtropical, monsoon climate zone	every 10min from 07:00 to 18:00 on 3 sunny days; leaf measured at intervals of 5-7 days
Zheng et al. [27]	grapevine	solar greenhouse under high latitude, cold, and high-radiation	from 21 May to 24 October (157 days), from 8 May to 4 November (177 days)
Harms [8]	tomato	Venlo-type soilless greenhouse	data recorded every 5min in a day (24h), transpiration period from 18 July to 13 September
Shao et al. [20]	tomato	Sunken solar greenhouse oriented north to south	daily and hourly scales from 1 November 2018 to 9 December 2020

## 1.2. Comparison between Transpiration Models

Until now, only a limited number of studies have been conducted to compare the performances of transpiration models under greenhouse conditions. Jolliet and Bailey [9] compared the estimated transpiration from the Penman, Stanghellini, Chalabi & Bailey, Aikman & Houter and Jolliet & Bailey models with the observed transpiration. The last three models are not really different models, just very similar models to the *PM* model using different calculations of canopy resistance ( $r_c$ ). They found that the Stanghellini and Jolliet & Bailey models performed best in quantifying tomato transpiration, as indicated by their higher Coefficient of Determination ( $R^2$ ) values (Table 1.3). Similarly, Prenger et al. [18] made a comparison of the performance of three different models, namely the Penman, Penman-Monteith and Stanghellini models, and found that the *SM* model provided the best results for predicting transpiration in Red Sunset Maple based on its higher  $R^2$  values (Table 1.3).

The Stanghellini model is generally considered to be the most accurate model for predicting

## 1. Introduction

transpiration under greenhouse conditions. However, the Penman-Monteith model is more widely used than the Stanghellini model, even under greenhouse conditions [15]. According to the above-mentioned studies, there is still a lack of information on comparing the performance of the **PM** and **SM** models for predicting tomato transpiration in greenhouses. In order to determine whether the Penman-Monteith model can provide reliable results comparable to the Stanghellini model, the performance of these two models will be evaluated and compared in the present study.

Table 1.3.: Results of Different Transpiration Models

Author	Crop	Model	Slope	R2
Jolliet and Bailey [9]	Tomato	Penman	Unknown	0.59
		Stanghellini	Unknown	0.77
		Chalabi & Bailey	Unknown	0.57
		Aikman & Houter	Unknown	0.73
		Jolliet & Bailey	Unknown	0.81
Prenger et al. [18]	Red Sunset Maple	Penman	Unknown	0.214
		Penman-monteith	Unknown	0.481
		Stanghellini	Unknown	0.872

### 1.3. Objectives of the Study

The **PM** and **SM** models are commonly used for predicting transpiration in greenhouse conditions. However, the assumption of homogeneity of micrometeorological parameters in these models, which is acceptable for open field conditions, may not be applicable for greenhouse crops due to the presence of artificial heating and ventilation system. These factors can introduce temperature gradients and humidity variations within the greenhouse. Consequently, it becomes crucial to determine the appropriate height of observation for microclimate parameters to accurately adapt the models to the specific climatic conditions of the greenhouse. Moreover, as the **SM** model is thought to provide better performance in greenhouse conditions, it is necessary to determine whether the **SM** model can actually offer more accurate transpiration estimates and whether the **PM** model can yield results equally reliable to the **SM** model. Therefore, the objective of the present study is to address the following points:

- Can the **PM** and **SM** models provide accurate transpiration estimations?
- Can the **PM** model yield results as reliable as the **SM** model?
- What is the optimal observation height for temperature data utilized in both models?



## 2. Methodology

### 2.1. Transpiration Model Theory

#### 2.1.1. Penman-Monteith model

The PM model combined the energy balance with the mass transfer method. At present, this method is widely recognized as one of the most established methods for computing transpiration ( $E_t$ ) [7]. The latent heat flux caused by crop transpiration is expressed as [3]:

$$\rho\lambda E_t = 3.6 \times 10^6 \times \frac{sR_n + C_p \rho_a \frac{(e_s - e_a)}{r_a}}{s + \gamma \left(1 + \frac{r_c}{r_a}\right)} \quad (2.1)$$

Where:

- $E_t$  transpiration ( $mm \cdot h^{-1}$ )
- $\lambda$  latent heat flux of vaporisation ( $J \cdot kg^{-1}$ ) ( $2.45 MJ \cdot kg^{-1}$ )
- $R_n$  netradiation ( $W \cdot m^{-2}$ )
- $C_p$  specific heat of air at constant pressure ( $J \cdot kg^{-1} \cdot K^{-1}$ ) ( $1004 J \cdot kg^{-1} \cdot K^{-1}$ )
- $\rho$  density of water ( $kg \cdot m^{-3}$ ) ( $1000 kg \cdot m^{-3}$ )
- $\rho_a$  density of air ( $kg \cdot m^{-3}$ )
- $e_a$  actual vapour pressure of the air ( $kPa$ )
- $e_s$  saturated vapour pressure of the air ( $kPa$ )
- $\gamma$  psychrometer constant ( $kPa \cdot K^{-1}$ ) ( $0.066 kPa \cdot K^{-1}$ )
- $r_a$  aerodynamic resistance ( $s \cdot m^{-1}$ )
- $r_c$  canopy resistance ( $s \cdot m^{-1}$ )
- $s$  slope of the saturated vapour pressure curve ( $kPa \cdot K^{-1}$ ), see Equation 2.3

$e_s$  is the maximum vapour pressure of water particles before condensation.  $e_s$  is a function of the temperature ( $T$ ). The empirical approximation provided by Moene and Van Dam [12] for calculating  $e_s$  in [ $kPa$ ] is given by:

$$e_s(T) = 0.6112e^{\frac{17.62(T-273.15)}{-30.03+T}} \quad (2.2)$$

## 2. Methodology

T temperature (K)

Where:

The slope of the saturated vapour pressure curve ( $s$ ) in [ $kPa \cdot K^{-1}$ ] can be easily determined from the derivative of Equation 2.2 [12]:

$$s = \frac{de_s}{dT} = e_s(T) \frac{4284}{(-30.03 + T)^2} \quad (2.3)$$

The advantage of this formula is that only one temperature input is required for the calculation of transpiration. This feature makes it particularly suitable for situations where there is limited temperature variation in the greenhouse.

### 2.1.2. Stanghellini model

The Stanghellini model has been specifically designed for greenhouse conditions. This model includes the LAI to account for energy exchange from multiple layers of leaves on the greenhouse crop. The equation for  $E_t$  in [ $mm/h$ ] is defined by Stanghellini [21] and described as follows:

$$\rho \lambda E_t = 3.6 \times 10^6 \times \frac{sR_n + C_p \rho_a \frac{2LAI(e_s - e_a)}{r_a}}{s + \gamma \left(1 + \frac{r_c}{r_a}\right)} \quad (2.4)$$

Where:

LAI leaf area index (–)

### 2.1.3. Aerodynamic Resistance

The aerodynamic resistance ( $r_a$ ) represents the resistance to the transfer of heat and water vapor from the evaporating surface into the air above the canopy [3]. To determine the  $r_a$  for the Penman-Monteith model and Stanghellini model models, the heat exchange coefficient ( $h_s$ ) induced by the airflow was used [23].

$$r_a = \frac{\rho_a C_p}{h_s} \quad (2.5)$$

Where:

$h_s$  heat exchange coefficient ( $W \cdot m^{-2} \cdot K^{-1}$ )

The Nusselt number is a dimensionless similarity parameter to describe convective heat transfer. Based on the flat plate theory, the value of  $h_s$  is expressed as a function of the  $N_u$  [15].

$$h_s = \frac{N_u \lambda_a}{l} \quad (2.6)$$

Where:

$N_u$  Nusselt number (-)

$\lambda_a$  air thermal conductivity ( $W \cdot m^{-1} \cdot K^{-1}$ )

$l$  characteristic dimension of the leaf ( $m$ )

According to Montero et al. [14], the calculation for characteristic dimension of the leaf ( $l$ ) can be expressed as follow:

$$l = \frac{2}{\frac{1}{L} + \frac{1}{W}} \quad (2.7)$$

Where:

$L$  length of the leaf ( $m$ )

$W$  Width of the leaf ( $m$ )

Convective conditions can be distinguished by Reynolds number ( $Re$ ) and Grashof number ( $Gr$ ).

$$Re = \frac{\rho_a u l}{\mu_a} \quad (2.8)$$

$$Gr = \frac{g \times \beta \times \Delta T \times l^3 \times \rho_a^2}{\mu_a^2} \quad (2.9)$$

## 2. Methodology

Where:

Re	Reynolds number (–)
u	wind speed ( $m \cdot s^{-1}$ )
$\mu_a$	air dynamic viscosity ( $Pa \cdot s$ )
Gr	Grashof number (–)
g	acceleration of gravity ( $m \cdot s^{-2}$ ) ( $9.81 m \cdot s^{-2}$ )
$\beta$	volumetric thermal expansion coefficient of air ( $K^{-1}$ )
$\Delta T$	temperature difference between the leaf temperature and the air temperature (K)

The expressions for  $N_u$  can be seen in Table [15].

Table 2.1.: Expression of the  $N_u$

Free $Re^2 \ll Gr$	Laminar $10^4 < Gr < 10^9$	$N_u = 0.54Gr^{\frac{1}{4}}$
	Turbulent $10^9 < Gr < 10^{12}$	$N_u = 0.12Gr^{\frac{1}{3}}$
Mixed $Re^2 \approx Gr$	Laminar $10^3 < Gr < 10^9$	$N_u = 0.68 \left( Re^{\frac{3}{2}} + Gr^{\frac{3}{4}} \right)^{\frac{1}{3}}$
	Turbulent $10^9 < Gr < 10^{12}$	$N_u = 0.03 \left( Re^{\frac{12}{5}} + 12.1Gr \right)^{\frac{1}{3}}$
Forced $Re^2 \gg Gr$	Laminar $3 \times 10^5 > Re$	$N_u = 0.56Re^{\frac{1}{2}}$
	Turbulent $5 \times 10^5 < Re$	$N_u = 0.03Re^{\frac{4}{5}}$

Free: Free convection arises from buoyancy forces resulting from density disparities induced by temperature fluctuations within a fluid.

Mixed: Mixed convection is a combination of forced and free convections.

Forced: Forced convection occurs when a fluid flow is induced by an external force

### 2.1.4. Canopy Resistance

The exchange of water vapor through the crop surface is affected by  $r_c$ , which is determined by the degree of stomatal aperture and is closely associated with the microclimate conditions. The larger the aperture, the smaller the resistance. To obtain the necessary resistance values, transpiration models were inverted and the resistance was deduced from measured transpiration rates. Canopy resistance can be modeled using a multiplicative function as follow [15]:

$$r_c = r_{c, min} f_1(R_n) f_2(VPD) f_3(T_a) \quad (2.10)$$

Where:

For a tomato crop, Katsoulas and Stanghellini [10] and Stanghellini [21] have demonstrated that the variations of  $r_c$  can be adequately described by two out of the three functions,

$r_{c, min}$	minimum canopy resistance ( $s \cdot m^{-1}$ )
VPD	vapour pressure deficit ( $kPa$ ) ( $VPD=e_s-e_a$ )
$T_a$	air temperature ( $K$ )

owing to the correlations between climatic parameters. Consequently,  $r_c$  can be formulated as a function of two variables, namely net radiation ( $R_n$ ) and vapour pressure deficit (VPD) [23]:

For the PM model:

$$r_c = c_1 \frac{R_n + c_2}{R_n + c_3} \left(1 + c_4 VPD_a^2\right) \quad (2.11)$$

For the SM model:

$$r_c = c_1 \frac{\frac{R_n}{2LAI} + c_2}{\frac{R_n}{2LAI} + c_3} \left(1 + c_4 VPD_a^2\right) \quad (2.12)$$

The values of  $c_1$  to  $c_4$  for a tomato crop were determined by Villarreal-Guerrero et al. [23] through an optimization procedure utilising the linear least squares in the surface fitting toolbox of Matlab (Table 2.2).

Table 2.2.: Values of  $c_1$  to  $c_4$

Model	Penman-Monteith model	Stanghellini model
$c_1$	0.35	18.6
$c_2$	9985	197.5
$c_3$	3.8	0.31
$c_4$	$2.61 \times 10^{-7}$	$1.2 \times 10^{-6}$

## 2.2. Experimental Method

As previously mentioned, the estimation of transpiration via PM and Stanghellini model (SM) models requires the input of various climatic parameters. This section describes the experimental setup that was implemented for the purpose of the study, as well as the corresponding measured parameters.

## 2. Methodology

### 2.2.1. Experimental Setup

The study was carried out in September in a Venlo-type greenhouse located at the Delphy Improvement Centre in Bleiswijk, South Holland. The experimental site lies within an oceanic climate zone and experiences an average temperature of around 16°C during this month. In September, Bleiswijk receives an average rainfall of 21.2 mm and approximately 5 days of rainfall, with humidity levels hovering around 68% [Online]. Different weather conditions caused large variability between the radiation intensity.

The greenhouse is rectangular in shape. The longer side has a southwest-to-northeast direction, which aligns with the prevailing wind direction. The greenhouse is naturally ventilated to allow for the exchange of hot and moist exhaust air from inside to outside and can be heated using a hot-water steel pipe heating system [8].

Mature Merlic tomato plants were used in the experiment, which is one of the main cultivars grown in the country. In total, there were 6 hanging gutters (14.7m × 0.25m) with a spacing of 1.6 m between the midpoints of adjacent gutters. Each gutter contains 11 slabs that each host 8 branches of the tomato plant. Each slab is 1.3 m in length and 0.15 m in width. Both control plants and experiment plants are in row 2. The mean bulk density and porosity of the Cultilene Exact Air rock wool slabs used were 50 kg/m<sup>3</sup> and 95 % respectively [8]. Two droppers were provided for each plant. Water was supplied to the plants depending on the radiation sum or an exceeding time span. No irrigation took place at night. The droppers were removed from the experiment slab on September 5. All plants received uniform agronomic management, including stem pruning, fertilization, pest control, and trellised support [8].

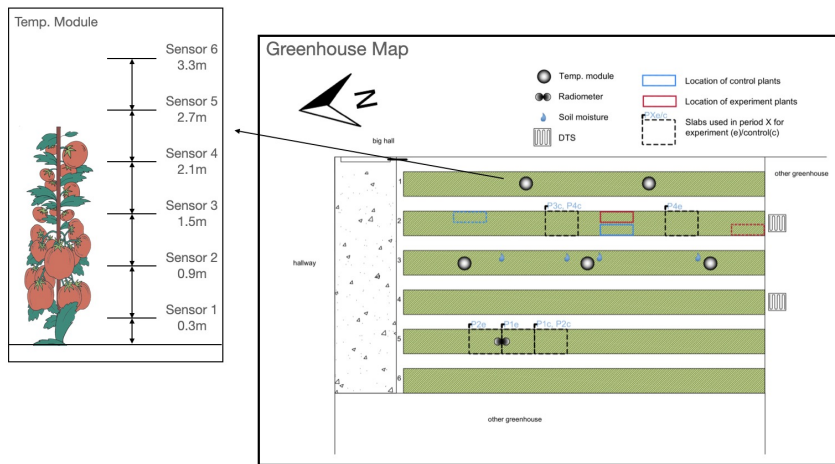
Following the FAO-56 approach, the growing season of the tomato crop is divided into four stages, namely: the initial stage, the crop development stage, the mid-season stage, and the late-season stage [1]. At the onset of the experiment, the plants were 8 months old and in the mid-season stage. Generally, tomatoes grow 20-30 cm a week. The branches were thus lowered and horizontally displaced throughout the gutter. This was also done to keep the top of the plants remains at the same point.

### 2.2.2. Microclimate Measurement

The microclimate parameters that were measured inside the greenhouse included net radiation ( $R_n$ ), air temperature ( $T_a$ ), leaf temperature ( $T_l$ ) and relative humidity ( $h$ ). A set of sensors were used to measure these microclimate parameters. The sensors of the experiment were installed between 30 August and 2 September. A schematic view of the experimental device is depicted in Figure 2.1, and a detailed description is provided in Table 2.3.

A CNR4 net radiometer with a sensitivity of 5 20 V · W<sup>-1</sup> · m<sup>-2</sup> [Zonen] was used to measure shortwave radiation and longwave radiation. In the CMOS integrated temperature module, air temperatures were measured at 0.3 m, 0.9 m, 1.5 m, 2.1 m, 2.7 m and 3.3 m heights from the ground. Air temperature and leaf temperature were also measured by leaf-to-air-temperature sensors (LAT). The sensors were placed at the root, middle and top of the plant.  $T_l$ ,  $h$ ,  $r_c$ , VPD, and  $E_t$  can be measured manually by LI-600 Porometer. All the data are averaged every 10 minutes.

## 2.2. Experimental Method



(a)

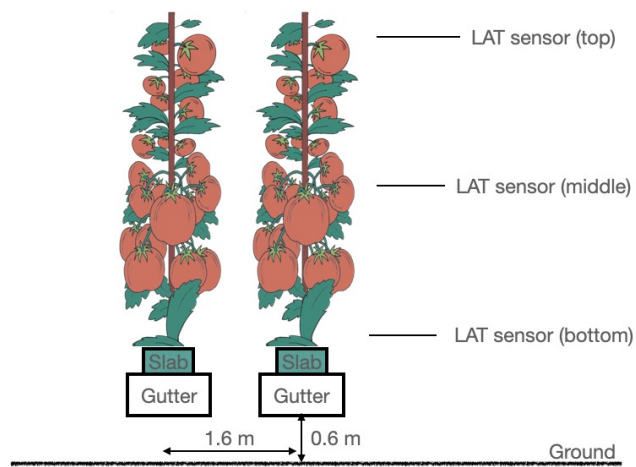


Figure 2.1.: Experimental Setup. (a) Temp. Module. (b) LAT.

## 2. Methodology

Table 2.3.: Devices for Measuring Microclimate Parameters

Sensor	Parameter	Detail
CNR4 net radiometer	$R_n$	Unit: $W \cdot m^{-2}$ Spectral range: 300 - 2800 $nm$ (short wave) 4500 to 42000 $nm$ (long wave) Sensitivity: $5 - 20 V \cdot s^{-1} \cdot m^{-2}$
CMOS integrated temperature module	$T_a$	Developed by Qinwen Fan as part as the Plantenna
Ecomatik LAT sensor	$T_a$ $T_l$	Unit: $^{\circ}C$ LAT_B2 (the bottom ones) LAT_B3 (all the others)
Poromoter	$T_l$	Unit: $^{\circ}C$ Operating conditions: 0 - 50 $^{\circ}C$ Accuracy: $\pm 0.5 C$
	VPD	Unit: % Operating conditions: 0 - 85%, non-condensing Accuracy: $\pm 2\% RH$
	$r_c$	Unit: $mol \cdot m^{-2} \cdot s^{-1}$
	VPD	Unit: $kPa$
	$E_t$	Unit: $mol \cdot m^{-2} \cdot s^{-1}$

### 2.2.3. Leaf Area Index Measurement

The leaf area index (**LAI**) is a dimensionless quantity that characterizes plant canopies. It is defined as a ratio of the leaf area to the ground area. Typically, **LAI** can be determined directly by taking a statistically significant sample from a plant canopy using a camera integrating system [24]. The **LAI** was assumed not to change significantly during our experiment period. A constant value of 3 was therefore used for the **SM** model, which is a commonly observed value for mature tomato crops [8].

### 2.2.4. Transpiration Measurement

Transpiration measurements are based on the concept of water balance:

$$\frac{dS}{dt} = Q_{in} - Q_{out} \quad (2.13)$$

Where:

- $Q_{in}$  incoming water flux
- $Q_{out}$  outgoing water flux
- $S$  storage



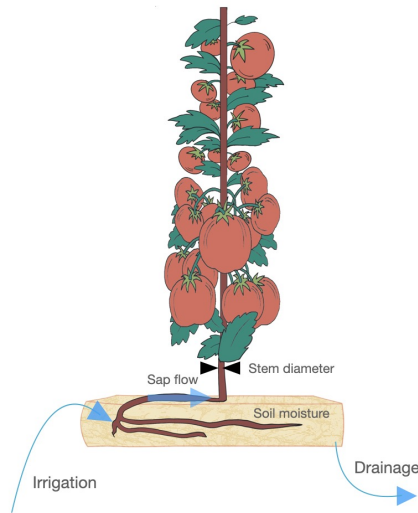


Figure 2.2.: Water Balance in the Slab

Figure 2.2 shows the water balance in the slab. In this study, the crops were watered through the irrigation system. Part of the water drains out through the gutter, while part is absorbed by the plants and finally evaporates through the leaves. Since the tomato crops were grown in rock-wool slabs covered with plastic, there is no evaporation from the slab. Also, part of the water may be stored in the soil to balance the difference between inputs and outputs. The water balance then reads:

$$\frac{dS_{soil}}{dt} = I - D - WE \quad (2.14)$$

Where:

- $S_{soil}$  soil moisture storage, which can be calculated through soil moisture
- $I$  irrigation
- $D$  drainage
- $WE$  water extraction by plant roots

In tomato crops, water balance can read:

$$\frac{dS_{plant}}{dt} = WE - E_t \quad (2.15)$$

Where:

## 2. Methodology

$S_{plant}$  water stored in the plants for growth

For simplification, water stored in the plants for growth is neglected. Transpiration in the tomato crop was then estimated by measuring the upward flow of sap from the root system to the leaf of a crop. During the day, the sap flow gives a good estimate of transpiration because a large amount of water passes directly through. When plants are well-watered, transpiration is roughly the same as the sap flow [2]. However, this method has a disadvantage at night, when sap flow is still present in the absence of transpiration.

The sap flow gauges were installed at representative plants of the tomato crop. The 2grow sap flow sensor was used to measure the sap flow and stem diameters. Sap flow and stem flow from September 9 to September 19 were measured, and these data were averaged every 10 min. The amount of irrigation and drainage water from each slab containing sap flow sampled plants was monitored using Priva water sensors. The data measured directly from sap flow sensors were compared daily to the water extraction values obtained via Priva water sensors (Equation 2.14).

Table 2.4.: Devices for Measuring Microclimate Parameters

Sensor	Parameter
2grow sap flow sensor	Sap flow
Priva water sensor	Irrigation Drainage
Teros	Soil moisture

## 2.3. Data Processing

### 2.3.1. Irrigation and Drainage

The data recorded in Excel was originally measured in units of  $L/m^2/h$ , representing the cumulative quantity of irrigation/drainage water for a duration of 5 minutes. To standardize the data, the raw values were first divided by 5. Subsequently, the data were further processed by calculating the mean value for each hour to mitigate the influence of short-term fluctuations. The final units for the irrigation/drainage water were expressed in  $mm/h$ .

### 2.3.2. Water Storage

Soil moisture content was determined by averaging measurements obtained from both the south and north sides of the control slab. The raw data was initially unitless. To calculate water storage, soil moisture values for each hour were selected. The water stored in the soil, expressed in  $mm$ , can be computed using Equation 2.16 as referenced below. Data for each hour were used for subsequent calculations.

$$water\ storage = \frac{bulk\ density\ (kg/m^3) \times soil\ moisture\ (-) \times slab\ volume\ (m^3) \times porosity\ (-)}{water\ density\ (kg/m^3) \times slab\ surface\ area\ (m^2)} \times 10^3 \quad (2.16)$$

### 2.3.3. Sap Flow

Sap flow data were collected at 10-minute intervals and expressed in  $g/h$ . Using Equation 2.17, the unit can be converted to  $mm/h$ . To facilitate further calculations, the sap flow values for each hour were averaged.

$$sap\ flow = \frac{sapflow\ (g/h)}{1000 \times slab\ surface\ area\ (m^2)} \quad (2.17)$$

### 2.3.4. Radiation and Temperature

Radiation and temperature data were measured at 10-minute intervals. Temperature measured at both the west and north side of the temperature module are averaged. To facilitate further calculations, the data for both variables were averaged for each hour.

## 2.4. Evaluation of Model Performance

The measured and calculated  $E_t$  were compared by linear regression analysis. Coefficient of Determination ( $R^2$ ) and slope were used to evaluate model performances and is expressed as:

$$R^2 = 1 - \frac{\sum_{i=1}^n (C_i - M_i)^2}{\sum_{i=1}^n (M_i - \bar{M})^2} \quad (2.18)$$

$$slope = \frac{\sum_{i=1}^n (M_i - \bar{M}) (C_i - \bar{C})}{\sum_{i=1}^n (M_i - \bar{M})^2} \quad (2.19)$$

Where:

- $C_i$  calculated transpiration
- $M_i$  measured transpiration
- $\bar{M}$  average measured transpiration

A better model performance has  $R^2$  value close to 1.

## 3. Result

### 3.1. Water Balance Model and Sap Flow

Given the limited availability of soil moisture data, the present study has opted to concentrate its analysis on the period between September 10 and September 19. Transpiration values calculated from the water balance model (Equation 2.15) were used to verify whether sap flow could be used as an indicator of transpiration.

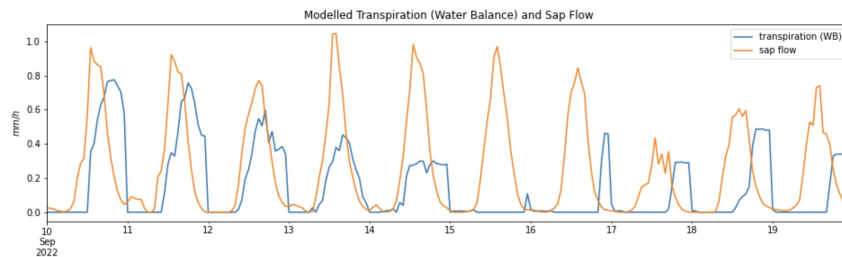


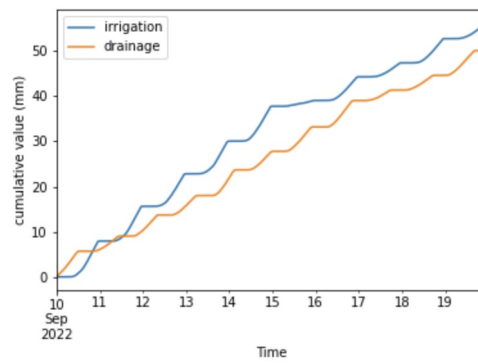
Figure 3.1.: Modelled Transpiration (Water Balance) and Sap Flow

Figure 3.1 illustrates the modelled transpiration and sap flow for tomato crops in September 2022. The water balance model used in this study includes a delay in estimating plant transpiration. This delay arises from the time required for water to move up to the leaves and evaporate into water vapor after its adsorption by the plant root system. Moreover, the storage dynamics within the soil and plant also introduce a delay in the model's transpiration estimates. Additionally, there is a time delay for the drainage water to reach the measurement point for drainage.

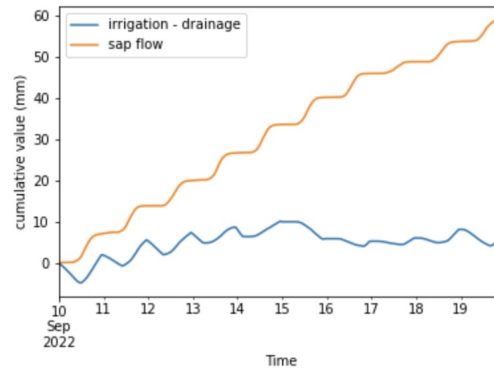
To mitigate the delay in estimating transpiration, daily total transpiration computed based on Water Balance model and sap flow rates were compared to evaluate the feasibility of using sap flow as a dependable indicator of transpiration.

Table 3.1.: Daily Modelled Transpiration and Sap Flow

Date	Transpiration (WB) (mm)	Sap Flow (mm)
9/10/22	7	7
9/11/22	6	7
9/12/22	5	6
9/13/22	4	7
9/14/22	4	7
9/15/22	0	6
9/16/22	1	6
9/17/22	2	3
9/18/22	3	5
9/19/22	2	5



(a) Irrigation and Drainage



(b) Water Extraction and Sap Flow

Figure 3.2.: Cumulative Graph)

The daily modeled transpiration rate was slightly lower than the daily sap flow rate, except for September 15 and 16, when a notably larger difference was observed. On average, the difference between the two rates was approximately 1.6 mm. As depicted in Figure 3.2, during these two days, the cumulative drainage rate exceeded the cumulative irrigation

### 3. Result

rate. This inconsistency could potentially be attributed to errors during the data collection and processing process.

A linear regression was conducted for the daily transpiration values and daily sap flow, with the exception of September 15 and 16.

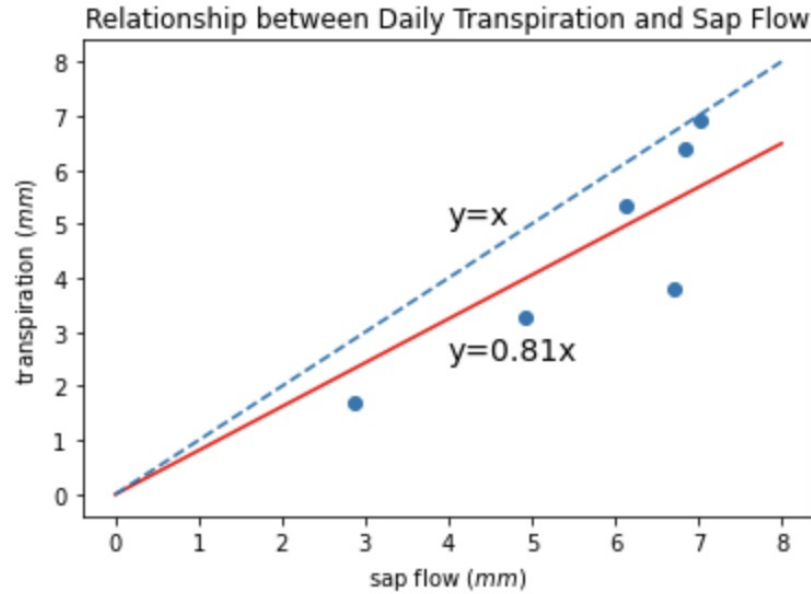


Figure 3.3.: Relationship between Daily Transpiration and Sap Flow

Sap flow includes water used for transpiration and water used for other plant functions, such as growth. Water stored in plants may also contribute to an increased sap flow rate. This is reflected in Figure 3.3, where the daily modelled transpiration is almost equivalent to 80% of the sap flow rate, with an  $R^2$  value of 0.86. Here, we use the 80% sap flow data to assess the ability of the PM and SM model to predict transpiration.

## 3.2. Microclimate Conditions

Microclimate parameters play a crucial role in the instantaneous variation of plant transpiration and are essential parameters for the accurate calculation of plant transpiration using PM and SM models.

### 3.2.1. Microclimate Data Measured by the Porometer

Several microclimate data were measured manually by Porometer from September 5 to September 9. Humidity varied from 43.86% to 73.73% and temperature varied from 21.52°C to 32.59°C. As shown in Figure 3.4, humidity is relative to the air temperature. An increase in temperature may result in a decrease in relative humidity, which can subsequently impact

plant transpiration rates. The microclimatic data shown in Figure 3.4 provide important fundamental information for the subsequent application of the PM and SM models to calculate transpiration.

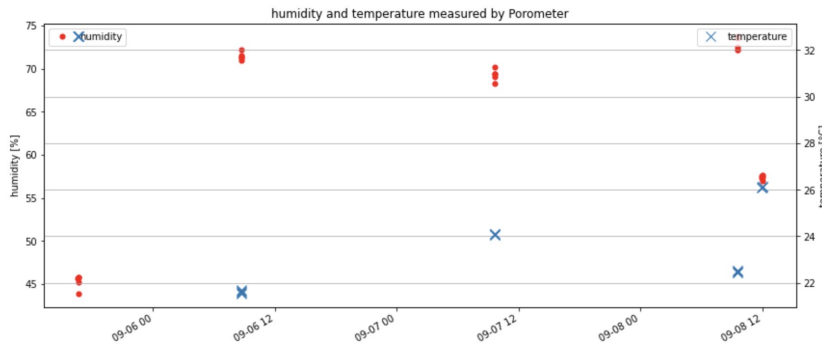


Figure 3.4.: Humidity and Temperature Measured by Porometer

### 3.2.2. Microclimate Data Measured by Other Devices

Some of the microclimate data were measured and recorded automatically by other devices from September 9 to September 22.

#### Temperature

Control plant 2B was well watered throughout the experiment and did not exhibit any signs of water stress. Leaf and air temperature were measured by LAT sensors at multiple locations, including near the roots (approx. 0.3 m) and at the top of the plant (approx. 2.3 m). The temperature fluctuations during this period are presented in the Figure 3.5. The air and leaf temperature obtained from the top and bottom of the plant didn't differ significantly. The average temperature during the period was around 21°C. This provides essential information to further determine the air properties required for the calculation of transpiration.

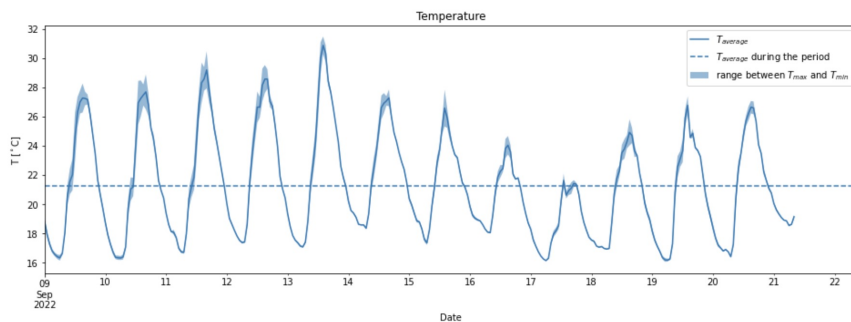


Figure 3.5.: Air Temperature Measured by LAT Sensors Plant 2B, at Height 0.3 and 2.3 m

### 3. Result

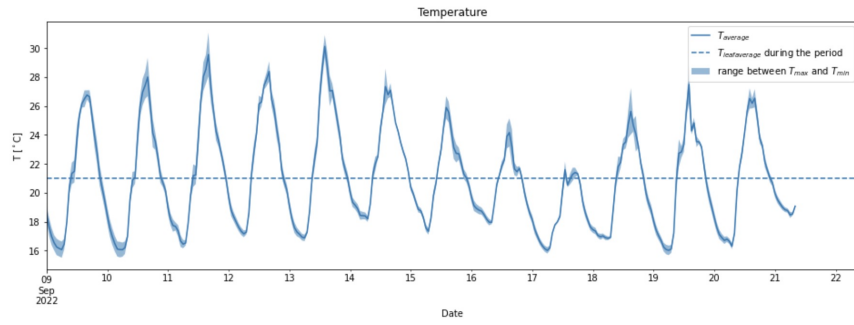


Figure 3.6.: Leaf Temperature Measured by LAT Sensors Plant 2B, at Height 0.3 and 2.3 m

### Radiation

As illustrated in the Figure 3.7, the net radiation ranged from  $1.68 \text{ W/m}^2$  to  $482.25 \text{ W/m}^2$  throughout the experimental period.  $R_n$  was close to zero during the night and increased during the day, showing a similar trend to temperature. On September 17, the net radiation remained much lower, indicating a cloudy day. This was consistent with the temperature trend fluctuations observed during the same period.

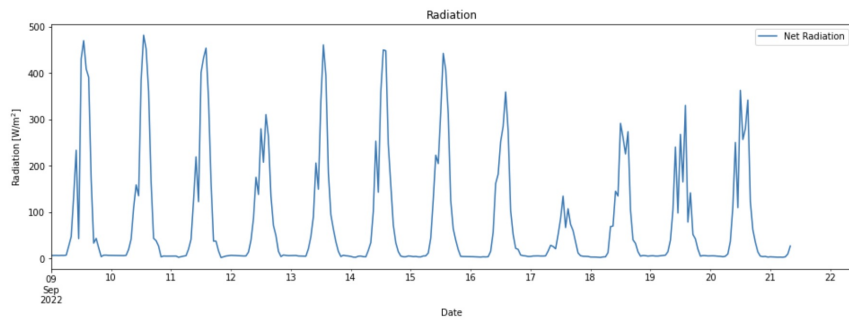


Figure 3.7.: Radiation Measurement

### 3.3. Aerodynamic and Canopy Resistance

Consistent with previous studies (Table 1.1), the resistance values were determined by Equation 2.5, Equation 2.11 and Equation 2.12 using air temperatures at the top of the plants.



### 3.3. Aerodynamic and Canopy Resistance

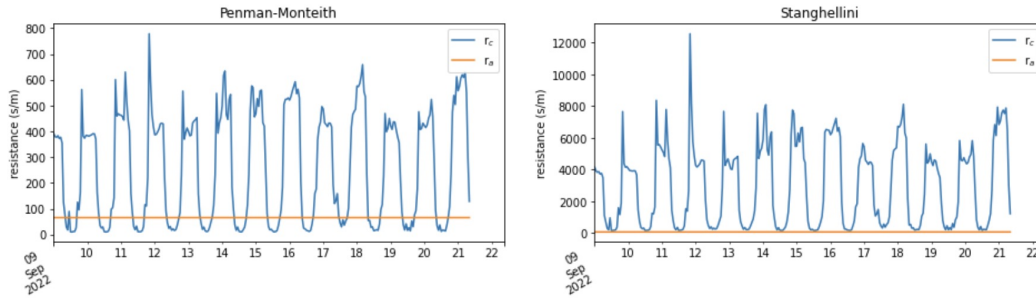


Figure 3.8.: Aerodynamic and Canopy Resistance

#### 3.3.1. Aerodynamic Resistance

Aerodynamic resistance is a critical parameter in the study of plant transpiration. It was calculated according to the heat exchange coefficient (Equation 2.5) using  $l = 0.043 \text{ m}$ , which is a typical value determined for tomatoes [23]. A wind speed of  $0.2 \text{ m/s}$  was assumed, which is a commonly used value in greenhouses under natural ventilation conditions [22]. The properties of the air for the computation of  $r_a$  are listed in the Table A.1. This method provides valuable information on the convective conditions of the airflow and the instantaneous variation of the  $r_a$ .

$Gr$  ranges between 3442888 and 3482289, with an average value of 3450190,  $Re^2$  is 323871. Based on these results, mixed convection is occurring between the canopy and air.

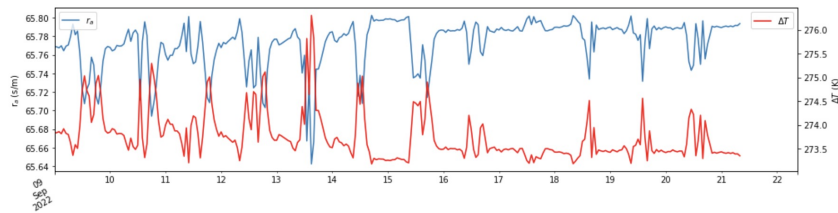


Figure 3.9.: Aerodynamic Resistance and Air-to-Leaf Temperature Difference

The results depicted in Figure 3.9 reveal that aerodynamic resistance varied slightly between  $65.6 \text{ s/m}$  and  $65.8 \text{ s/m}$ . Notably, during midday, when radiation reaching the plant induced a higher temperature difference between the leaf and air,  $r_a$  was observed to be lower. Moreover, as displayed in Figure 3.8, aerodynamic resistance remains relatively constant when compared to canopy resistance. It indicates that using a constant  $r_a$  does not result in a significant loss of accuracy in predicting transpiration. Our findings are in accordance with previous studies that have utilized a constant  $r_a$  to simulate transpiration [8].

#### 3.3.2. Canopy Resistance

The utilization of a constant canopy resistance may result in inaccurate predictions of transpiration due to the influence of  $VPD$  and  $R_n$  [9]. To address this issue, we calculated  $r_c$

### 3. Result

separately for the **PM** (Equation 2.11) and **SM** (Equation 2.12) models in our study. The values of the parameters  $c_1$  to  $c_4$  determined by Villarreal-Guerrero et al. [23] for tomato crops were used in the calculation of canopy resistance. Based on the information presented in Figure 3.4, a relative humidity value of 70% was selected to calculate canopy resistance at the average temperature of the greenhouse.

The impact of solar radiation on canopy resistance is considerable, leading to significant differences between the values of  $r_c$  at night and during the day. As shown in Figure 3.10, for the **PM** model, canopy resistance ( $r_c$ ) ranged from 10  $s/m$  during the day to 780  $s/m$  at night, while for the **SM** model, it varied from 148  $s/m$  during the day to 12553  $s/m$  at night. Notably, canopy resistances for the **SM** model are 10 times greater than those for the **PM** model, which is consistent with the findings of Villarreal-Guerrero et al. [23]'s research for tomato crops in a greenhouse environment.

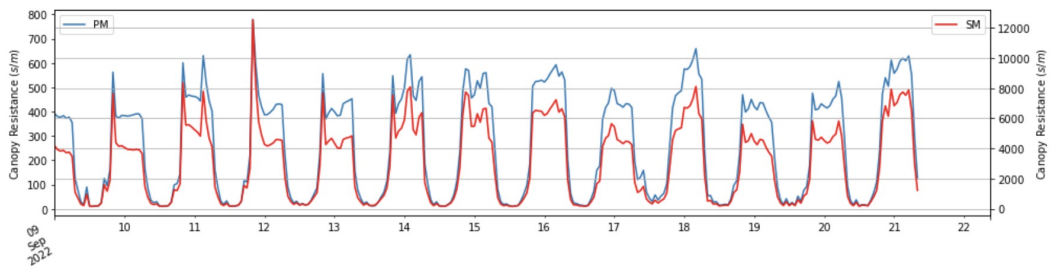


Figure 3.10.: Canopy Resistance

### 3.4. Application of the Penman-Monteith model and the Stanghellini model

Figure 3.11 depicts the measured and modelled hourly transpiration from September 9 to September 22. The measured transpiration was obtained from sap flow measurements. The modelled transpiration values were derived from the calculations of the Penman-Monteith model and Stanghellini model. In accordance with prior studies (Table 1.1), these models utilized air temperatures measured by the highest LAT sensor on plant 2B to estimate transpiration rates.

### 3.4. Application of the Penman-Monteith model and the Stanghellini model

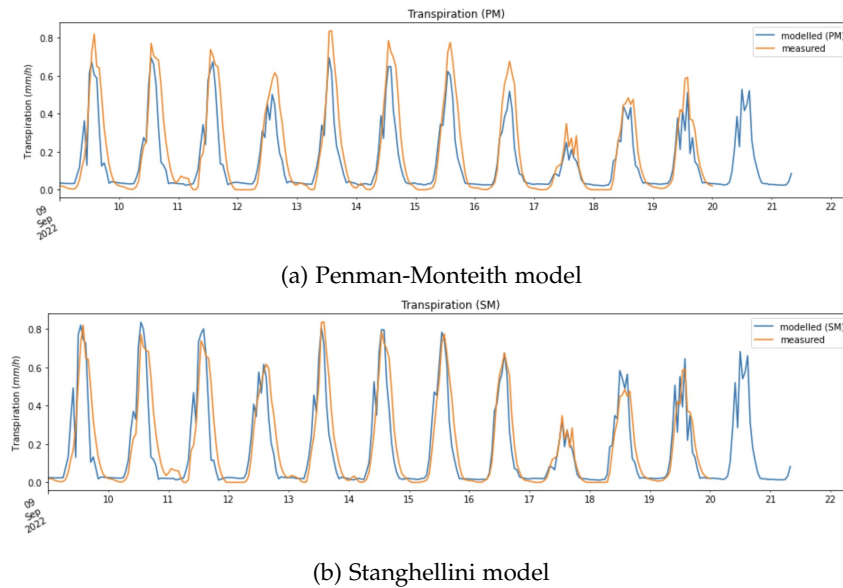


Figure 3.11.: Comparison between measured and estimated transpiration (T at top of plants)

As shown in Figure 3.11, for the PM model, significant underestimations of the transpiration rate are observed during the daytime. During the nighttime, the modelled transpiration overestimates the measured transpiration. The SM model provides relatively accurate estimates of the transpiration rates. However, the modelled transpiration rates also tend to be underestimated when there is a decrease in solar radiation.

To better assess the relationship between the measured and modelled values of the transpiration rate, the slope and Coefficient of Determination of the regression line were calculated. The results of these calculations are presented in Figure 3.12. For the PM model, the slope of the regression line is 0.73 and  $R^2$  is 0.768. For the SM model, the slope of the regression line is 0.89 and  $R^2$  is 0.777.

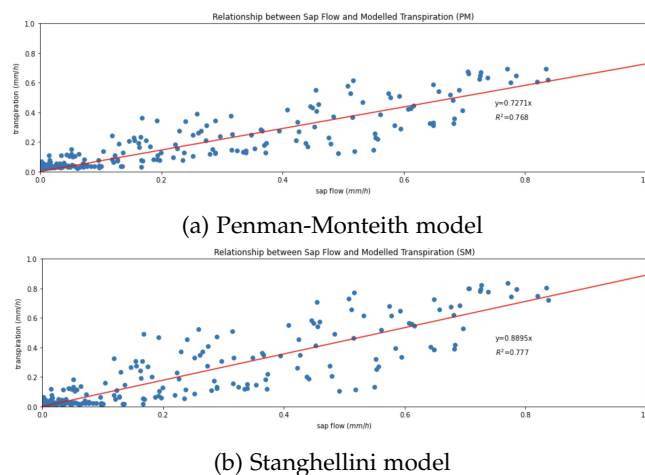


Figure 3.12.: Relationship between Sap Flow and Modelled Transpiration

### 3. Result

The slope of the regression line being closer to 1 for the **SM** model indicates a better agreement between the modelled transpiration and the measured values. Additionally, a higher  $R^2$  indicates a better overall fit of the model to the observed transpiration data. Therefore, based on the regression analyses, the **SM** model exhibits higher accuracy in predicting transpiration compared to the **PM** model. The observed trend of larger errors in the range of sap flow is between 0.4 to 0.6. The estimation of transpiration from midday to night shows relatively poor performance. It could be associated with the delay in sap flow decrease when transpiration decreases.

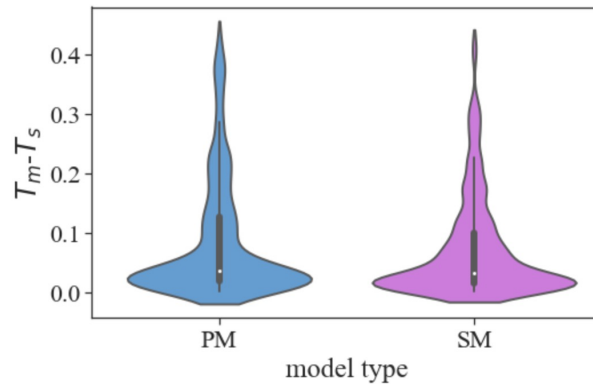


Figure 3.13.: Violin Graph

The violin [Figure 3.13](#) shows the difference between the modeled transpiration and sap flow, providing an insightful depiction of the distribution of errors for both the **PM** and **SM** models. The plot reveals that the majority of errors fall within the range of 0 to 0.1 for both models, indicating a relatively close agreement between the modeled transpiration and observed sap flow measurements.

## 3.5. Selection of the Optimal Temperature Measurement Locations

The selection of appropriate temperature measurement locations is crucial in accurately estimating transpiration rates for the **PM** and **SM** models. By carefully choosing the most suitable temperature measurement locations, more precise estimations of transpiration can be obtained. In this study, air temperature data were collected from six different locations. In the subsequent sections, the selection of the optimal temperature measurement locations for both the **PM** and **SM** models will be discussed.

### 3.5.1. Temperature Used in the Penman-Monteith model

For the **PM** model, the slope and coefficient of determination of the regression line between the measured and modelled transpiration values were calculated using a set of air temperatures. The results of these calculations are presented in [Table 3.2](#).

### 3.5. Selection of the Optimal Temperature Measurement Locations

Table 3.2.: Correlation between Measured and Simulated Transpiration Rates (PM)

Location (m)	Slope	R <sup>2</sup>
0.3	0.71	0.76
0.9	0.72	0.77
1.5	0.74	0.78
2.1	0.76	0.79
2.7	0.77	0.79
3.3	0.77	0.79

Temperature was measured in temperature module 0.3, 0.9, 1.5, 2.1, 2.7 and 3.3 m from plant roots

The selection of air temperatures at heights of 2.1 m, 2.7 m, and 3.3 m from the plant roots resulted in similar and better correlations. Therefore, using air temperature measured above the top of the plant canopy is deemed a suitable choice to serve as a parameter in the PM model.

#### 3.5.2. Temperature Used in the Stanghellini model

Table 3.3.: Correlation between Measured and Simulated Transpiration Rates (SM)

Location (m)	Slope	R <sup>2</sup>
0.3	0.85	0.78
0.9	0.88	0.78
1.5	0.93	0.78
2.1	0.99	0.75
2.7	1.00	0.74
3.3	1.00	0.75

Temperature was measured in temperature module 0.3, 0.9, 1.5, 2.1, 2.7 and 3.3 m from plant roots

The selection of air temperatures at heights of 2.1 m, 2.7 m, and 3.3 m from the plant roots has resulted in better correlations. Hence, using air temperatures above the top of the plant canopy as a parameter for the SM model is a suitable approach.

Using temperatures above the top of the plant canopy appears to be a reliable method for estimating transpiration in greenhouse conditions. This observation is consistent with prior research (Table 1.1).

## 4. Discussion

The objective of this study is to establish a precise model for estimating transpiration in greenhouse environments. This model is utilized to predict variations in transpiration rates within the greenhouse, thereby facilitating the improvement of water management strategies. The improved strategies are intended to mitigate water wastage by meeting the exact water requirements of plants for optimal growth and development.

To achieve this objective, several analyses and comparisons were conducted, as outlined below:

### 1. Comparison of daily sap flow and daily transpiration computed from the water balance model

The relationship between sap flow and daily transpiration computed by the water balance model was investigated. The analysis revealed that daily transpiration estimated by the model was consistently around 80% of the measured daily sap flow. Several reasons contribute to the discrepancies observed between sap flow values and model-based transpiration estimations.

- Sap flow measurements capture the movement of water within the plant. In addition to transpiration, water is transported for other purposes such as storage within the plants as well. This internal water movement contributes to the overall sap flow measurements but is not reflected in the transpiration estimated by the water balance model, leading to variations between sap flow values and model-based transpiration estimations.
- Sap flow measurements are directly obtained from the plant stems, while the water balance model estimates transpiration based on various factors, such as irrigation, drainage and soil moisture content measurements. Differences in measurement techniques or potential measurement errors can also contribute to variations between sap flow and model-based transpiration estimations.
- The water balance model relies on various assumptions. Humidity, wind speed and leaf area index were assumed to be constant values in this study. These assumptions may not fully capture the complex and dynamic nature of transpiration in real-world greenhouse conditions. Deviations from the actual conditions may lead to differences between the sap flow measurements and model-based transpiration estimations.
- The delay between drainage from the slab and measurement at the end of the gutter

Sap flow values tend to differ from the model-based transpiration values. In previous studies, sap flow was directly used as an indicator of measured transpiration, which may result in an incorrect estimation of actual transpiration. In the study, 80% of measured sap flow was utilized as an indicator of measured transpiration. This adjusted

approach can help us to select a transpiration model that more accurately reflects the realities observed in greenhouse conditions.

## **2. Comparison of Estimated Transpiration by the Penman-Monteith Model and Stanghellini Model with Measured Transpiration (Temperatures Measured at the Top of the Plant)**

The accuracy of the transpiration estimates using two models under greenhouse conditions was evaluated by comparing the measured transpiration with the transpiration estimated by the Penman-Monteith and Stanghellini models. In this analysis, temperatures obtained at the top of the plant were utilized as inputs for both models. The performance of the models was assessed based on the slope value and the coefficient of determination.

The results of the analysis demonstrated that the Stanghellini model exhibited a slope value closer to 1 and a higher  $R^2$  compared to the Penman-Monteith model. This indicates a stronger correlation between the estimated transpiration and the measured transpiration, and a better overall fit of the model to the observed data. Therefore, it can be concluded that the Stanghellini model outperformed the Penman-Monteith model in estimating transpiration under greenhouse conditions. The better performance of the Stanghellini model can be attributed to several factors.

- The Stanghellini model is specifically designed to account for the characteristics of greenhouse environments. It incorporates crop characteristic factors, such as leaf area index, which have a significant impact on transpiration rates. In contrast, the penman-monteith model is a more generalized transpiration model that may not fully capture the specific conditions present in greenhouses.

By considering crop characteristic parameters, the Stanghellini model allows for more accurate estimations of transpiration compared to the Penman-Monteith model. This finding emphasizes the importance of considering crop characteristics, such as LAI, in improving the accuracy of transpiration estimation.

## **3. Comparison of Estimated Transpiration by the Penman-Monteith Model and Stanghellini Model with Measured Transpiration (Temperatures Measured at Different Vertical Locations)**

To investigate the influence of vertical temperature distribution on transpiration estimation, temperatures were measured at six different heights within the greenhouse. These measured temperatures were used to estimate transpiration in the Penman-Monteith and Stanghellini models. By comparing the measured values with the estimated values, it was observed that temperatures measured above the top of the plant canopy provided more accurate estimations of transpiration for both models. This finding can be attributed to several reasons.

- Transpiration rates are typically higher in the upper canopy due to the higher exposure of leaves to solar radiation and the increased transpiration demand. Using temperatures measured above the top of the canopy enables a closer approximation of the actual transpiration rates in the greenhouse.

The findings of this study provide further evidence supporting the notion that incorporating temperatures measured above the top of the plant canopy leads to improved accuracy in transpiration estimation for both the Penman-Monteith and Stanghellini

#### 4. Discussion

models. This finding is consistent with previous studies, which highlighted the significance of considering the vertical temperature distribution in estimating transpiration in greenhouse conditions.

#### 4. Limitations

- In the present study, it was observed that the water balance model assumes that all water extracted by the plants is transpired, without accounting for potential output such as leaf surface evaporation and water storage within the plants. This simplification in the model may lead to an overestimation of transpiration estimates based on the model. It is crucial to incorporate other relevant factors to improve the accuracy of transpiration estimation models in future research.
- Due to the limited availability of information, this study utilized constant values for humidity, leaf area index, and wind speed. The use of these constant values may have introduced potential inaccuracies in the estimation of transpiration. To enhance the precision of future transpiration estimations, it is recommended to incorporate more realistic values for these parameters.



## 5. Conclusion

This study aimed to evaluate the accuracy of transpiration estimations using the Penman-Monteith and Stanghellini models under greenhouse conditions. The findings reveal that the Stanghellini model provides more accurate estimations of transpiration compared to the Penman-Monteith model. Measuring temperatures above the top of the plant canopy enhances the accuracy of transpiration estimations in both models. Future research should focus on addressing the limitations of the water balance model and incorporating more realistic parameter values to further improve the accuracy of transpiration estimation models in greenhouse conditions.



# A. Appendix

## A.1. Greenhouse Setup

Figure A.1 is a brief description of the slab.



Figure A.1.: Slab

## A.2. Air Properties

Air properties can be seen in [Table A.1](#) [6].

Table A.1.: Air Properties

Air properties	Unit	Values
density of air ( $\rho_a$ )	$kg \cdot m^3$	1.2047
air dynamic viscosity ( $\mu_a$ )	$Pa \cdot s$	$1.8205 \times 10^{-5}$
volumetric thermal expansion coefficient of air ( $\beta$ )	$K^{-1}$	$3.43 \times 10^{-3}$

### A.3. Selection of the Optimal Temperature Measurement Locations

#### 0.3 m from plant roots

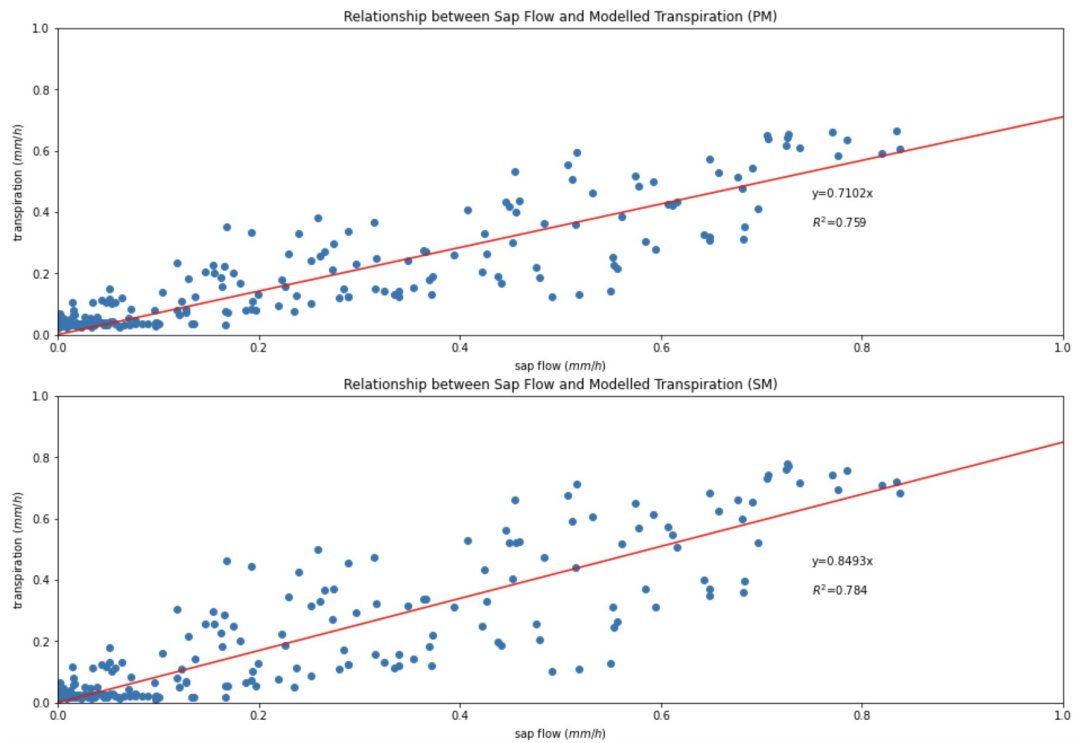


Figure A.2.: 0.3 m from plant roots

#### 0.9 m from plant roots

### A.3. Selection of the Optimal Temperature Measurement Locations

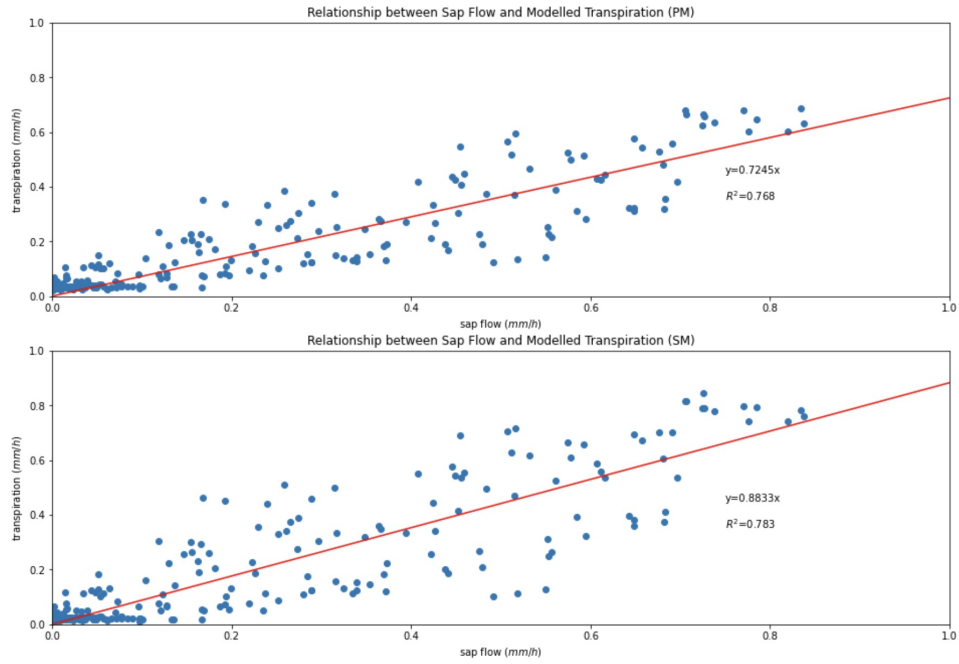


Figure A.3.: 0.9 m from plant roots

### 1.5 m from plant roots

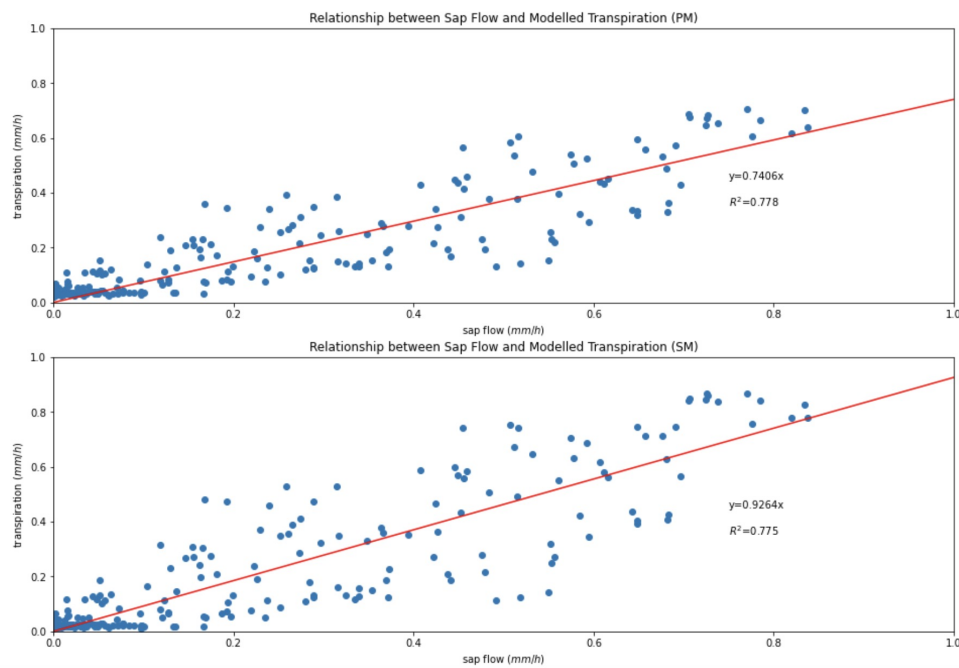


Figure A.4.: 1.5 m from plant roots

A. Appendix

2.1 m from plant roots

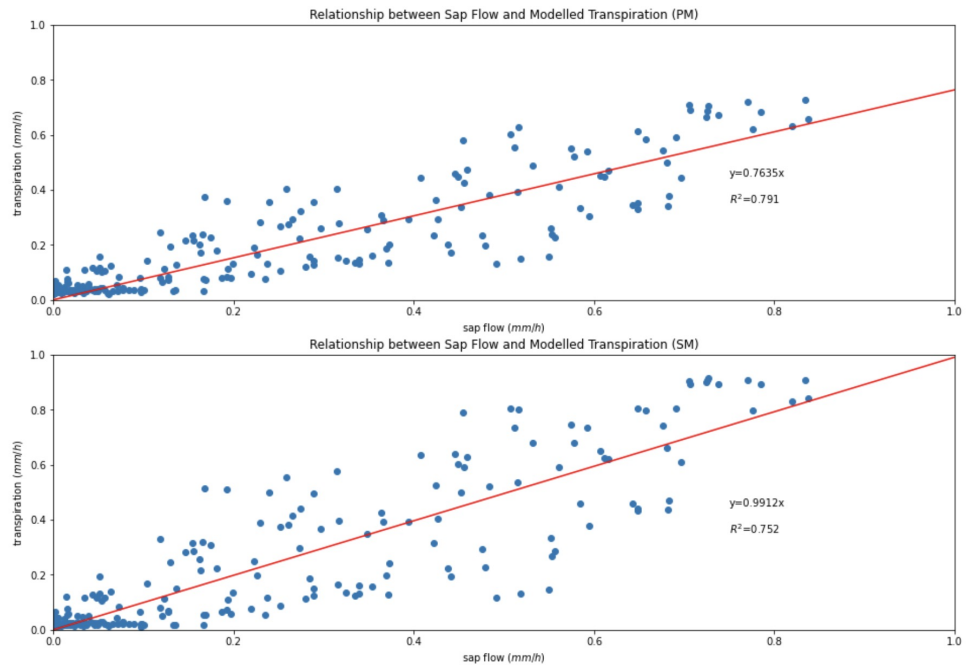


Figure A.5.: 2.1 m from plant roots

2.7 m from plant roots

### A.3. Selection of the Optimal Temperature Measurement Locations

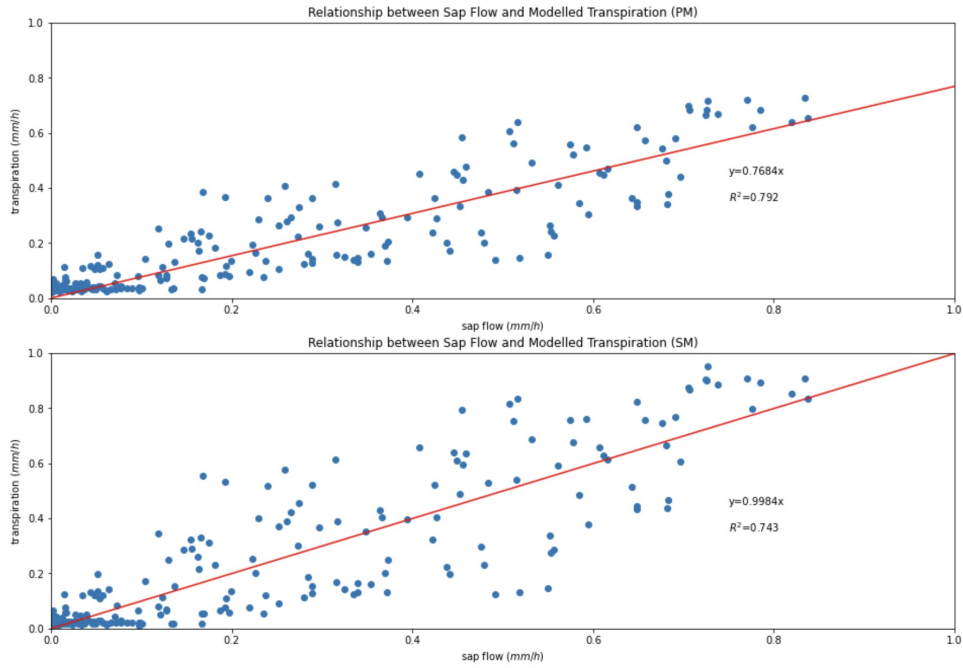


Figure A.6.: 2.7 m from plant roots

3.3 m from plant roots

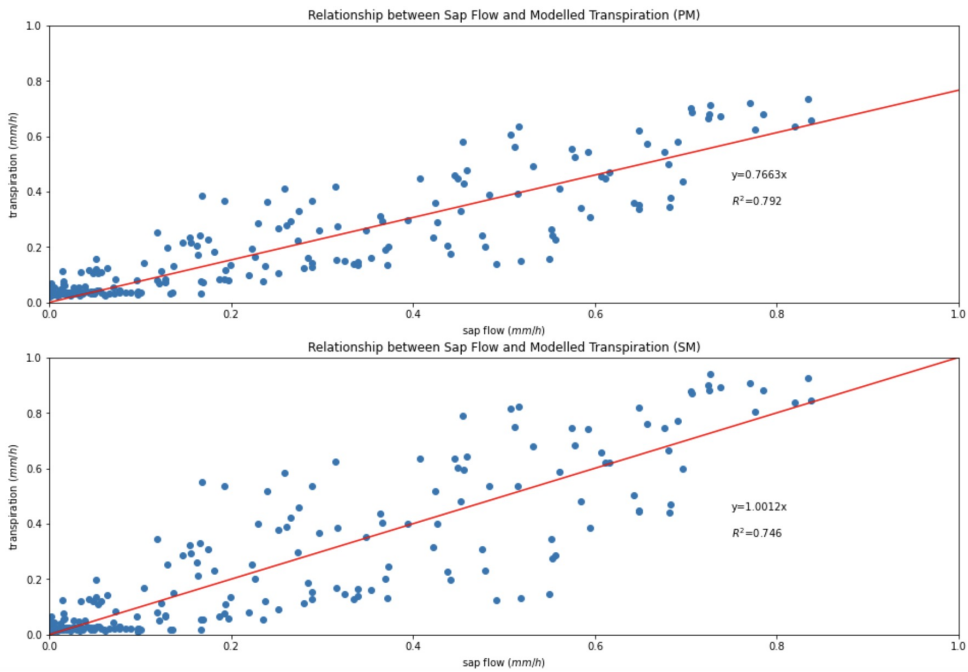


Figure A.7.: 3.3 m from plant roots

## Bibliography

- [1] Acquah, S. J., Yan, H., Zhang, C., Wang, G., Zhao, B., Wu, H., and Zhang, H. (2018). Application and evaluation of stanghellini model in the determination of crop evapotranspiration in a naturally ventilated greenhouse. *International Journal of Agricultural and Biological Engineering*, 11(6):95–103.
- [2] Alarcón, J., Domingo, R., Green, S., Sánchez-Blanco, M., Rodríguez, P., and Torrecillas, A. (2000). Sap flow as an indicator of transpiration and the water status of young apricot trees. *Plant and Soil*, 227:77–85.
- [3] Allen, R. G., Pereira, L. S., Raes, D., Smith, M., et al. (1998). Crop evapotranspiration-guidelines for computing crop water requirements-fao irrigation and drainage paper 56. *Fao, Rome*, 300(9):D05109.
- [4] Bailey, B., Montero, J., Biel, C., Wilkinson, D., Anton, A., and Jolliet, O. (1993). Transpiration of ficus benjamina: comparison of measurements with predictions of the penman-monteith model and a simplified version. *Agricultural and Forest Meteorology*, 65(3-4):229–243.
- [5] Caspari, H., Green, S., and Edwards, W. (1993). Transpiration of well-watered and water-stressed asian pear trees as determined by lysimetry, heat-pulse, and estimated by a penman-monteith model. *Agricultural and Forest Meteorology*, 67(1-2):13–27.
- [6] Evans, P. (March 29, 2015). Properties of air at atmospheric pressure. <https://theengineeringmindset.com/properties-of-air-at-atmospheric-pressure/>.
- [7] Hao, X., Zhang, S., Li, W., Duan, W., Fang, G., Zhang, Y., and Guo, B. (2018). The uncertainty of penman-monteith method and the energy balance closure problem. *Journal of Geophysical Research: Atmospheres*, 123(14):7433–7443.
- [8] Harms, K. (2022). An analysis of four different models for quantifying tomato transpiration in a soilless greenhouse.
- [9] Jolliet, O. and Bailey, B. (1992). The effect of climate on tomato transpiration in greenhouses: measurements and models comparison. *Agricultural and Forest Meteorology*, 58(1-2):43–62.
- [10] Katsoulas, N. and Stanghellini, C. (2019). Modelling crop transpiration in greenhouses: different models for different applications. *Agronomy*, 9(7):392.
- [11] Lee, J. W., Kang, W. H., Moon, T., Hwang, I., Kim, D., and Son, J. E. (2020). Estimating the leaf area index of bell peppers according to growth stage using ray-tracing simulation and a long short-term memory algorithm. *Horticulture, Environment, and Biotechnology*, 61:255–265.
- [12] Moene, A. F. and Van Dam, J. C. (2014). *Transport in the atmosphere-vegetation-soil continuum*. Cambridge University Press.



- [13] Monteith, J. L. (1965). Evaporation and environment. In *Symposia of the society for experimental biology*, volume 19, pages 205–234. Cambridge University Press (CUP) Cambridge.
- [14] Montero, J., Antón, A., Muñoz, P., and Lorenzo, P. (2001). Transpiration from geranium grown under high temperatures and low humidities in greenhouses. *Agricultural and Forest Meteorology*, 107(4):323–332.
- [15] Morille, B., Migeon, C., and Bournet, P.-E. (2013). Is the penman–monteith model adapted to predict crop transpiration under greenhouse conditions? application to a new guinea impatiens crop. *Scientia Horticulturae*, 152:80–91.
- [Online] Online, W. W. Bleiswijk annual weather averages. <https://www.worldweatheronline.com/bleiswijk-weather-averages/south-holland/nl.aspx>.
- [17] Penman, H. L. (1948). Natural evaporation from open water, bare soil and grass. *Proceedings of the Royal Society of London. Series A. Mathematical and Physical Sciences*, 193(1032):120–145.
- [18] Prenger, J., Fynn, R., and Hansen, R. (2002). A comparison of four evapotranspiration models in a greenhouse environment. *Transactions of the ASAE*, 45(6):1779.
- [19] Salokhe, V., Babel, M., Tantau, H., et al. (2005). Water requirement of drip irrigated tomatoes grown in greenhouse in tropical environment. *Agricultural water management*, 71(3):225–242.
- [20] Shao, M., Liu, H., and Yang, L. (2022). Estimating tomato transpiration cultivated in a sunken solar greenhouse with the penman-monteith, shuttleworth-wallace and priestley-taylor models in the north china plain. *Agronomy*, 12(10):2382.
- [21] Stanghellini, C. (1987). *Transpiration of greenhouse crops: an aid to climate management*. Wageningen University and Research.
- [22] Teitel, M., Ziskind, G., Liran, O., Dubovsky, V., and Letan, R. (2008). Effect of wind direction on greenhouse ventilation rate, airflow patterns and temperature distributions. *Biosystems Engineering*, 101(3):351–369.
- [23] Villarreal-Guerrero, F., Kacira, M., Fitz-Rodríguez, E., Kubota, C., Giacomelli, G., Linker, R., and Arbel, A. (2012). Comparison of three evapotranspiration models for a greenhouse cooling strategy with natural ventilation and variable high pressure fogging. *Scientia Horticulturae*, 134:210–221.
- [24] Wikipedia (2022). Leaf area index. [https://en.wikipedia.org/wiki/Leaf\\_area\\_index#cite\\_note-10](https://en.wikipedia.org/wiki/Leaf_area_index#cite_note-10).
- [25] Wikimedia (2023). Greenhouse. <https://en.wikipedia.org/wiki/Greenhouse>.
- [26] Yan, H., Huang, S., Zhang, C., Gerrits, M. C., Wang, G., Zhang, J., Zhao, B., Acquah, S. J., Wu, H., and Fu, H. (2020). Parameterization and application of stanghellini model for estimating greenhouse cucumber transpiration. *Water*, 12(2):517.
- [27] Zheng, S., Wang, T., and Wei, X. (2021). Estimating grapevine transpiration in greenhouse with three different methods in a penman–monteith model in northeast china. *Irrigation Science*, pages 1–15.
- [Zonen] Zonen, K. . Cnr4 net radiometer. [www.kippzonen.com/Product/85/CNR4-Net-Radiometer#.ZDbu\\_S86E\\_U](http://www.kippzonen.com/Product/85/CNR4-Net-Radiometer#.ZDbu_S86E_U).

## **Colophon**

This document was typeset using  $\text{\LaTeX}$ , using the KOMA-Script class `scrbook`. The main font is Palatino.

